Adaptive optics confocal microscopy using fluorescent protein guide-stars for brain tissue imaging

Xiaodong Tao*[a], Oscar Azucena [a], Min Fu [c], Yi Zuo [c], Diana C. Chen[b], Joel Kubby [a]
[a]W.M. Keck Center for Adaptive Optical Microscopy, Jack Baskin School of Engineering, Univ. of California, Santa Cruz, Santa Cruz, CA, USA 95064;
[b]Lawrence Livermore National Laboratory, 7000 East Avenue, Livermore, CA, USA 94550;
[c]Molecular, Cell, and Developmental Biology, Univ. of California, Santa Cruz, CA, USA 95064

ABSTRACT

Optical aberrations due to the inhomogeneous refractive index of tissue degrade the resolution and brightness of images in deep tissue imaging. We introduce a direct wavefront sensing method using cellular structures labeled with fluorescent proteins in tissues as guide-stars. As a non-invasive and high-speed method, it generalizes the direct wavefront sensing method for adaptive optics microscopy. An adaptive optics confocal microscope using this method is demonstrated for imaging of mouse brain tissue. The confocal images with and without correction are collected. The results show increased image contrast and 3X improvement in the signal intensity for fixed mouse tissues at a depth of 70 μm. The images of the dendrite and spines are much clearer after correction with improved contrast. The Strehl ratio is improved from 0.29 to 0.96, a significant 3.3X improvement.
Keywords: Adaptive optics, confocal microscopy, wavefront sensor, wavefront correction, deep tissue imaging

1. INTRODUCTION

Optical microscopes have been widely used in biological science because of their ability to resolve cellular structures. And the advances in super resolution techniques can even extend the resolution to near molecular level [1]. However the optical imaging depth is still limited. The resolution of the system is degraded with the imaging depth. One of the important reasons is the optical aberration induced by the inhomogeneous optical properties of the biological samples and the refractive index mismatch between the sample and mounting medium. Although most commercial high magnification objectives are equipped with correction collars, they are only optimized for compensation of the spherical aberration induced by the cover plate. It is impossible to correct the dynamic aberration induced by a live sample. To correct the aberrations, adaptive optics (AO) have been applied in various optical microscopes [2,3]. The performance of the wavefront correction in terms of accuracy and speed largely depends on the wavefront measurement. Although wavefront sensors have been widely used in adaptive optics system in astronomy, the requirement of a guide-star reference beacon limits its application in microscopy. Most of the existing adaptive optics (AO) microscopes developed so far are based on indirect methods of wavefront measurement which depends on processing of the final image [3,4]. Those systems require numerous iterations to find the wavefront parameters. The extended exposure time will cause photo-bleaching and limits the bandwidth for live imaging. Other approaches use a direct wavefront measurement, but use a serial operation [5] based on sequential measurements of the wavefront error in each segment of the aperture [6, 7], or sequential intensity measurements with different trial aberrations [8]. Both of these serial approaches will be too slow for live imaging. We have demonstrated a direct wavefront measurement method with parallel operation [5], where a fluorescent microsphere injected into the sample was used as a reference source for a Shack-Hartmann wavefront sensor (SHWS)[9, 10]. The exposure time during wavefront sensing is much shorter than the indirect wavefront methods [3, 4] and the serial approaches [6, 7, 8], which reduces the possibility of photo-toxicity and photo-bleaching. It also enables higher speed imaging for dynamic live samples. However, this method requires the injection of fluorescent microspheres into the sample, which complicates the sample preparation procedure. As an invasive method, the side effects of injection to the functionality of biological tissue need to be considered for live imaging.

*taoxd@soe.ucsc.edu

To overcome these disadvantages and generalize the direct wavefront sensing method, fluorescent proteins are used as a laser guide-star in this paper. Green fluorescent protein (GFP) has good photostability and high quantum yields which makes it a good candidate as a laser guide-star in AO microscopy. As a noninvasive fluorescent marker, the GFP has been extensively used in live cell imaging. AO microscopy can be easily applied to those studies without special preparation of the samples. The possible damage to the sample because of injection of a bead can be avoided. In this paper, the genetic mutant of GFP, yellow fluorescent protein (YFP) was investigated for wavefront measurement.

2. MATERIALS AND METHOD

2.1 System setup and operation principle

Figure 1 (a) shows the system diagram. The YFP in the sample is excited by a solid state laser (λ=515nm, Cobolt Fandango). Two galvo scanners (6215H, Cambridge Technology) provide raster scanning and beam parking for confocal imaging and guide-star illumination, respectively. The emission light is collected by a 60X water immersion objective with a numerical aperture of 1.2 (Olympus Microscope, Center Valley, PA). In order to measure the wavefront using the light from the guide-star, a 50/50 beam splitter splits the emission light from the YFP into a Shack-Hartmann wavefront sensor (SHWS) and a photo-multiplier tube (PMT) (H4022-50, Hamamatsu). To minimize the intensity loss from the division of light by the BS, a modified system with a switchable mirror instead of the beam splitter is under development to maximize the signal into the PMT or the wavefront sensor. A pinhole is mounted on the PMT to block the light from outside of the focal plane. The size of the pinhole is 1 Airy Unit (AU), which gives the best signal/noise ratio. The SHWS is composed of a 44x44 element lenslet array with a lens diameter of 400 μm and focal length of 24 mm (AOA Inc., Cambridge, MA) and an electron multiplying (EM) CCD camera (Cascade II, Photometrics). The pupil size on the wavefront sensor is 4mm, which will cover 76 lenslets. To estimate the wavefront error, a cross-correlation centroiding algorithm and a Fast Fourier Transform (FFT) reconstruction algorithm were implemented using Visual C++ [11, 12]. In order to minimize the amount of out of focus light that enters the SHWS, an iris is placed in the light path. The iris also blocks stray light from the DM, scanner and lenses. The iris acts as a low pass spatial filter, which will block the higher order wavefront. However it will only give a small contribution to the overall aberration. For mouse brain tissue, the first 12 Zernike modes (without piston, tip, and tilt) contribute the most aberration. The size of the pinhole can be determined from the bandlimit of the wavefront measurement. According to [13], 12 lenslets are the minimum number of lenslets for a reliable measurement of those aberrations. The measured wavefront is bandwidth limited at $1/2d_{sub}$ because of aliasing [14], where d_{sub} is the width of the subaperture. A spatial filter with width of λ/d_{sub} can attenuate the high-spatial frequency content above $1/2d_{sub}$. With the aperture of 4mm, d_{sub} for 12 lenslets is 0.94μm. The angular size of the spatial filter is 5.6×10^{-4} rad, which corresponds to a pinhole size of 140μm at I in Figure 1 (a). The experimental setup is shown in Figure 1 (b). The AO system was integrated into an Olympus IX71 inverted microscope (Olympus Microscope, Center Valley, PA) through its side optical port.

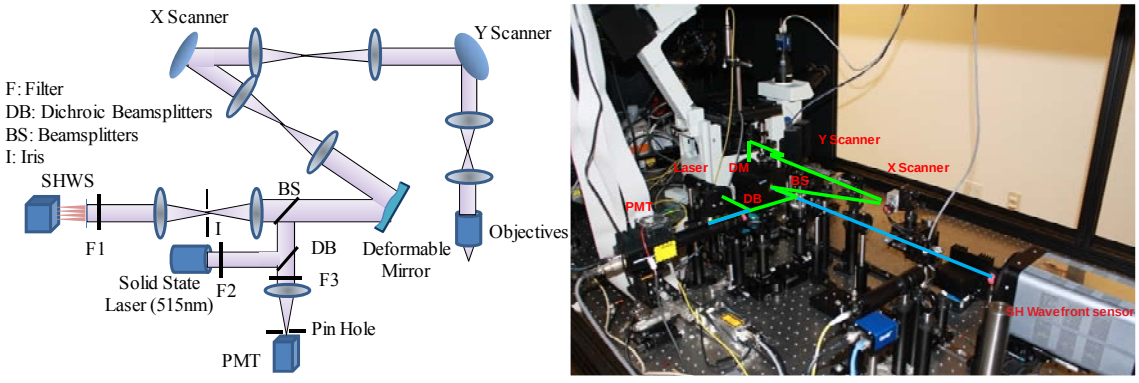

(a) (b)

Figure 1. System Layout (a) and experimental setup (b) of the Adaptive Optics Confocal Microscope.

2.2 Specimen preparation

Mice were used in accordance with protocols approved by the UCSC Institutional Animal Care and Use Committee. The YFP-H mouse was deeply anesthetized by ketamine-xylazine mixture and perfused intracardially using 0.1 mole phosphate buffer followed with 4% paraformaldahyde (PFA). The whole brain was dissected and post-fixed in 4% PFA overnight. Then a vibrotome was used for slicing the brain into different thickness. The brain slices were mounted on Colorfrost®Plus slide (Fisher Scientific) using the Fluoromount-G™mounting medium (CELL LAB).

2.3 Wavefront Sensing using fluorescent protein guide-stars

The SHWS consists of a lenslet array and a CCD camera. The local tilt of the wavefront on each lenslet can be estimated from the displacement of the focal spot on the sensor. The whole wavefront error can then be reconstructed from the local slopes. The diffraction limited spots on the sensor are required to make an accurate estimation. Therefore the diameter of the guide-star should be smaller than the diffraction limit of the wavefront sensor defined as [15]:

$$d_{diffraction\_limit} = 2.44 \frac{\lambda}{2NA} \frac{D_0}{d_l} \tag{1}$$

where λ is the wavelength, NA and D_0 are the numerical aperture and the pupil diameter of the objective, respectively. d_l is the diameter of a lens in the Shack-Hartmann lenslet array. In most of the cases, the diffraction limit of the wavefront sensor is much larger than that of the microscope system. In our current setup, $d_{diffraction\_limit}$ is equal to 5.36 µm. When using fluorescent protein as guide-stars, the size of the guide-star is limited by the illumination point spread function (PSF) because the fluorescent light from a given point is proportional to the light intensity illuminating that point. Based on the wavefront measurement for the brain tissue in [10], the PSF can be estimated through a Fourier transform [16]. For brain tissue at a depth of 70 µm, the diameter of the PSF with 80% of the encircled energy is 1.4 µm, which is small enough to be used as a guide-star.

In order to collect enough photons on the wavefront sensor, the laser focal point is fixed on the region of the YFP, which may cause photo-bleaching in a short amount of time if the laser power is too high. In this system, the laser power was set to 23nw at the back aperture of the objective lens during wavefront sensing. The worst case is tested where YFP in a dendrite with a lower concentration of fluorophores was used as a guide-star. Confocal images are obtained every 30 sec during the exposure of the laser. The normalized intensity change in the focal area and the image of the spot pattern on the wavefront sensor are shown in Figure 2. After the first 3 minutes, the intensity only drops less than 10%. However the exposure time for one wavefront measurement is only 500ms. The total exposure time for a closed-loop correction with 10 iterations is 5 seconds. The exposure time can be decreased by increasing the laser power, which will provide the same number of photons for wavefront sensing. For the structures with more fluorophores, such as a cell body, the exposure time can be much shorter.

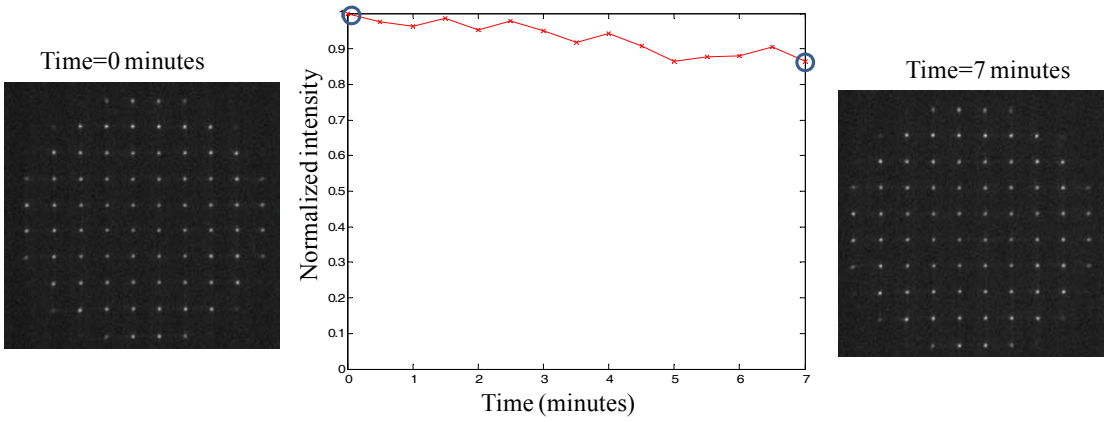

Figure 2. Normalized intensity at the focal point on the dendrite and spot pattern on the SHWS for photo-bleaching analysis.

The noise of the wavefront sensor is related to the signal to noise ratio (SNR) of the camera. In our current setup, the number of photons per subaperture using the parameters above are around 2000 counts with a read noise of 55e-/pixel, 200x EM gain and negligible dark current. The SNR is round 45. Using Equation 2, the RMS measurement error can be estimated as follows [5]:

$$\sigma_m = \sqrt{2}\frac{\pi^2 K_g}{4(SNR)}\left[\left(\frac{3}{2}\right)^2 + \left(\frac{\theta d}{\lambda}\right)^2\right] \tag{2}$$

where K_g =1.3 is a constant to account for centroiding errors due to the fill factor on the CCD. $\theta = 1.8\times10^{-3}$ rad is the angular radius of the spot size. $\lambda = 0.527$ μm is the wavelength. d=400μm is the subaperture diameter. The RMS measurement error is around 0.03 λ.

3. RESULTS

3.1 Wavefront measurements using the fluorescent protein guide-stars on different structures

To show the ability to measure the wavefront using fluorescent protein guide-stars, different structures of YFP in mouse brain tissue are tested. Figure 3 (a) and (d) show the dendrite and cell body of the neuron that were used as laser guide-stars at depths of 20 μm and 60 μm, respectively. The red cross lines show the locations of the laser focus. Figure 3 (b) and (e) are spot patterns on the SHWS. As can be seen, the size of the structure does not affect the wavefront measurement. The size of the guide-star depends on the point spread function of the optical system, which is much smaller than the diffraction limit of the wavefront sensor. Because the cell body shown in Figure 3(d) is deeper than the dendrite in Figure 3(a), the spot pattern has more spherical distortion, as shown in Figure 3(e). The exposure time of the wavefront measurement for the dendrite and cell body are 500 ms and 50 ms, respectively. Because the dendrites have less fluorophores than the cell bodies, longer exposure times are required for accurate wavefront measurement. The wavefront measurements are shown in Figure 3 (c) and (f). The RMS wavefront errors are 0.15λ and 0.23λ, respectively.

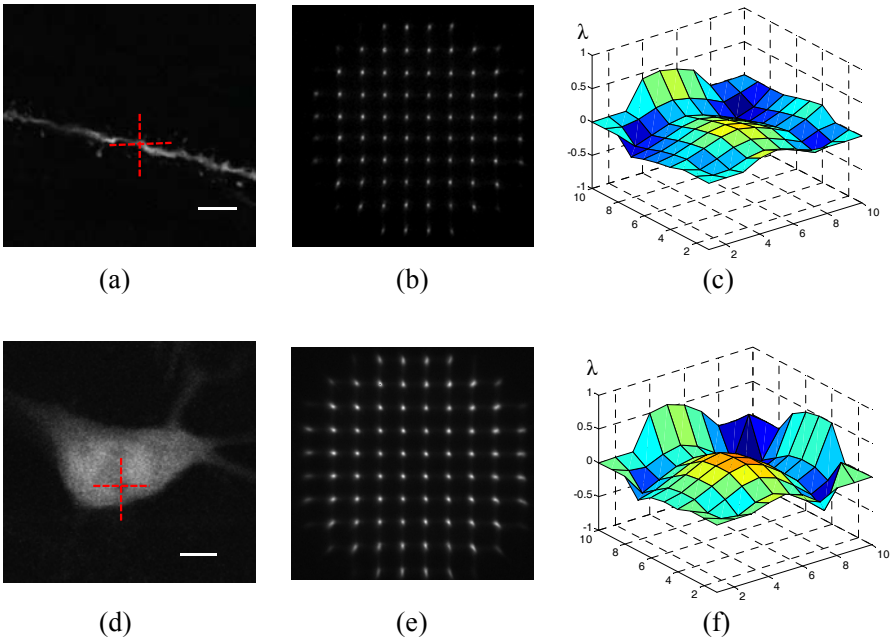

Figure 3. Wavefront measurements using the fluorescent protein guide-stars on a dendrite (a) and on a cell body (d). Figure (b) and (c) are the spot patterns on the SHWS and the wavefront error estimation for the fluorescent protein guide-stars on a dendrite, respectively. Figure (e) and (f) are the spot pattern on the SHWS and the wavefront error estimation for the fluorescent protein guide-stars on cell body, respectively. The scale bars are 5 μm. The crossed lines indicate the location of the focus point.

3.2 Wavefront correction using the fluorescent protein guide-stars

The confocal images before correction and after correction are shown in Figures 4 (a) and (d). The confocal images are collected by scanning along the z axis with a 3 μm range and 0.15 μm step size. The maximum intensity projection is applied to achieve the final image. The YFP in the cell body is used as a guide-star, which is located at a depth of 70μm. The exposure time for one measurement is 30ms. It takes around 10 iterations to close the loop to correct the aberration. The wavefront errors before correction and after correction are shown in Figures 4 (c) and (f). It shows that the RMS wavefront error decreased from 0.35λ to 0.034λ. The images after correction are much brighter than the ones before correction. The details of the image in the rectangular box are shown in Figures 4 (b) and (e). The intensity profile along the dashed lines across a dendrite and a spine is shown in Figure 4 (f). The peak intensity increases by 3x. The image of the dendrite and spines are much clearer after correction with improved contrast. The Strehl ratio is improved from 0.29 to 0.96, a significant 3.3x improvement.

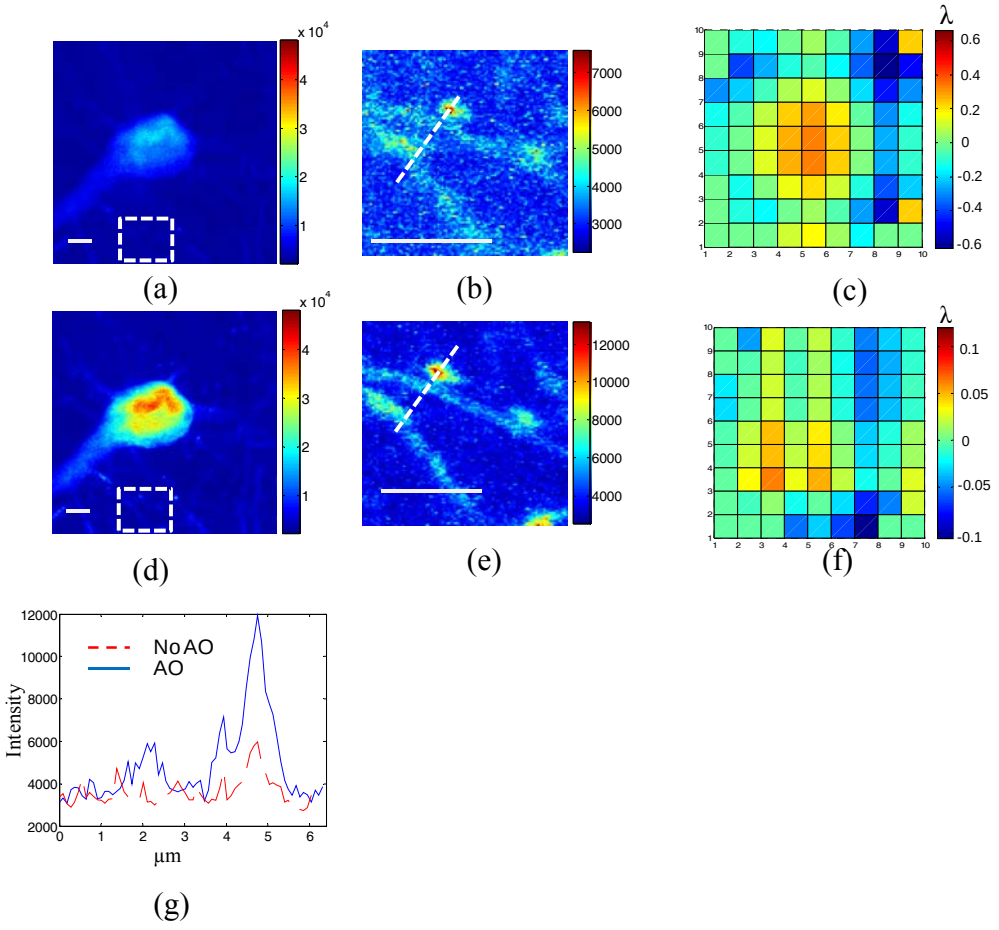

Figure 4. Wavefront correction using the fluorescent protein guide-stars on the cell body. The confocal images without AO (a) and with AO (d). The enlarged image in the rectangular box without AO (b) and with AO (e). The wavefront error without AO (c) and with AO (f). Intensity profiles (g) along the dashed line in (b) and (e). The scale bar is 5 μm.

4. CONCLUSION

We have demonstrated using fluorescent proteins labeled in sub-cellular structures as reference guide-stars for measuring wavefront aberrations, which generalizes the direct wavefront sensing technique to many different samples, especially for live *in-vivo* imaging. The optimization of the wavefront measurement speed and laser power density with minimal photobleaching will be investigated. The

synchronization method between wavefront error correction and confocal imaging will be developed for imaging of dynamic live samples.

ACKNOWLEDGMENTS

This material is based upon work supported by the National Science Foundation (NSF) under Award No. 0852742 and the W. M. Keck Center for Adaptive Optical Microscopy at UC, Santa Cruz.

REFERENCES

[1] Ji, N., Shroff, H., Zhong, H. and Betzig, E., "Advances in the speed and resolution of light microscopy", Curr. Opin. Neurobiol. **18**, 605–616 (2006).

[2] Debarre,D., Botcherby, E. J., Watanabe,T. Srinivas, S., Booth,. M. J. and Wilson,T. "Image-based adaptive optics for two-photon microscopy", Opt. Lett. **34**, 2495–2497 (2009).

[3] Marsh, P., Burns, D. and Girkin, J., "Practical implementation of adaptive optics in multiphoton microscopy", Opt. Express **11**, 1123–1130 (2003).

[4] Albert, O., Sherman, L., Mourou, G., Norris, T.B. and Vdovin, G., "Smart microscope: an adaptive optics learning system for aberration correction in multiphoton confocal microscopy", Opt. Lett. **25**, 52-54 (2000).

[5] Hardy, J. W., Adaptive Optics for Astronomical Telescopes, Oxford University Press, (1998).

[6] Ji, N., Milkie, D. and Betzig, E., "Adaptive optics via pupil segmentation for high-resolution imaging in biological tissues", Nature Methods **7**, 141 - 147 (2009).

[7] Milkie, D., Betzig, E. and Ji, N., "Pupil-segmentation-based adaptive optical microscopy with full-pupil illumination", Optics Letters **36**, 4206-4208 (2011).

[8] Booth, M., Neil, M., Juskaitis, R. and Wilson, T., "Adaptive aberration correction in a confocal microscope". Proc. Natl Acad. Sci. USA. **99**, 5788–5792 (2002).

[9] Azucena, O., Crest, J., Kotadia, S., Sullivan, W., Tao, X., Reinig, M., Gavel, D., Olivier, S. and Kubby, J., "Adaptive optics wide-field microscopy using direct wavefront sensing", Opt. Lett. **36**, 825-827 (2011).

[10] Tao, X., Fernandez, B., Azucena, O., Fu, M., Garcia, D., Zuo, Y., Chen, C. D. and Kubby, J., "Adaptive optics confocal microscopy using direct wavefront sensing", Opt. Lett. **36**, 1062-1064 (2011).

[11] Poyneer, L. A., Gavel, D. T. and Brase, J.M., "Fast wave-front reconstruction in large adaptive optics systems with use of the Fourier transform," J. Opt. Soc. Am. A **19**, 2100–2111 (2003).

[12] Thomas, S., Fusco, T., Tokovinin, A., Nicolle, M., Michau, V. and Rousset, G., "Comparison of centroid computation algorithms in a Shack-Hartmann sensor," Mon. Not. R. Astron. Soc. **371**, 323–336 (2006).

[13] Porter, J., Queener, H., Lin, J., Thorn, K. and Awwal, A.A.S, "Adaptive Optics for Vision Science: Principles, Practices, Design and Applications", Wiley (2006).

[14] Poyneer, L. A. and Macintosh, B. A., "Spatially filtered wave-front sensor for high-order adaptive optics", Opt. Soc. Am. A **21**, 810–819 (2004).

[15] Azucena, O., Tao, X., Crest, J., Kotadia, S., Sullivan, W., Gavel, D., Reinig, M., Olivier, S. and Kubby, J., "Adaptive optics wide-field microscope corrections using a MEMS DM and Shack-Hartmann wavefront sensor", Proc. SPIE **7931**, 79310J (2011).

[16] Beverage, J., Shack, R. and Descour, M., "Measurement of the three-dimensional microscope point spread function using a Shack–Hartmann wavefront sensor", J. Microscopy **205**, 61-75 (2002).